

# LTE Random Access Detection Based on a CA-CFAR Strategy

Felipe A. P. de Figueiredo, José A. Bianco F., Karlo G. Lenzi, Fabbryccio A. C. M. Cardoso, Onésimo Ferreira, and Fabrício L. Figueiredo

DRC – Convergent Networks Department  
CPqD – Research and Development Center  
Campinas, SP - Brazil

{felipep, jbianco, klenzi, fcardoso, onesimof, fabricio}@cpqd.com.br

**Abstract** — Random Access is an important aspect of mobile systems where multiple users are always competing for resources. However, noise imposes a significant problem to those systems causing them to falsely detect access requests. In consequence, unnecessary processing and air traffic are generated based upon these unreal request events. This paper presents a modified Cell-Average Constant False Alarm Rate (CA-CFAR) strategy used for random access detection of CAZAC preambles in the presence of noise. Simulation results indicate that the proposed method performs well even in the case of low SNR.

**Keywords:** CA-CFAR, CAZAC, LTE, PRACH, Random Access, Signal Detection, Zadoff-Chu Sequence.

## I. INTRODUCTION

The Random Access Channel (RACH) in Long Term Evolution (LTE) systems is mainly used for User Equipment (UE) to request resources from Base Station (BS) [4]. In the physical random access channel (PRACH) Zadoff-Chu (ZC) sequences are adopted as preambles. This adoption is based on the fact that the ZC sequences present ideal auto-correlation and cross-correlation properties [1-3]. Different ZC sequences or the same ZC sequence with different cycle shifts are used for generating preambles by different User Equipment (UE) [5, 6].

When detecting random access requests from users in a mobile network, the task of a Random Access Detector is to decide whether only noise or request(s)-plus-noise are present.

A RACH detector typically determines if an access to the network is been requested based upon statistical computations. The results from this statistical analysis are employed to calculate a threshold value that is then used to decide whether there is a user requesting access or not. Correct selection of the threshold is very important once the threshold determines the probability of false alarm, as well as the probability of detection [10].

It is of extreme necessity to determine a threshold value that produces both low alarm rate and good detection rate. However, the uncertainty of the noise variance is an important problem for the determination of a proper threshold. There are some techniques for the reducing the noise effect [12]. One of them is the Cell-Averaging Constant False-Alarm Rate (CA-CFAR) method. CA-CFAR detectors have been proposed in

[13] and [14] and consist of two steps: removing of the corrupted reference cells, also known as censoring, and the actual detection. In CA-CFAR detection, the detection threshold is the sum of the squared noise-only reference samples multiplied by a scaling factor [7]. In the case of wireless channels where the noise statistics are unknown, constant false alarm rate (CFAR) strategies can be used. Therein the detection threshold is determined by using reference sets.

In this paper, a modified version of the CA-CFAR method is presented and assessed. It is employed for detecting the presence of preamble sequences in the random access channel. The remainder of this work is organized as follows. Section II briefly describes the structure of the LTE signal. Section III introduces both the PRACH receiver structure adopted for user detection and the energy measurement the proposed method relies on. In Section IV, a modified version of a CA-CFAR detector is proposed. Results are presented and discussed in Section V. Finally, Section VI gives the conclusions.

## II. LTE SIGNAL STRUCTURE

The LTE standard is based on Orthogonal Frequency Division Multiple Access (OFDMA) to reach high data rates and data volumes. High order modulation (up to 64QAM), large bandwidth (ranging from 1.25 MHz and up to 20 MHz) and Multiple Input Multiple Output (MIMO) transmission schemes in the downlink (up to 4x4) is also a part of the standard. The highest theoretical data rate is 170 Mbps in uplink and with MIMO the rate can be as high as 300 Mbps in the downlink [8].

In order to achieve higher radio spectral efficiency, a multicarrier approach for multiple accesses is employed. OFDMA is used as the downlink modulation scheme and Single Carrier - Frequency Division Multiple Access (SC-FDMA) also known as DFT (Discrete Fourier Transform) spread OFDMA is used as the uplink scheme.

### A. LTE Generic Frame Structure for FDD

Figure 1 shows the LTE Generic Frame Structure for Frequency Domain Duplexing (FDD) [9]. As can be seen, LTE frames are 10 [ms] long. They are divided into 10 sub-frames with each sub-frame being 1.0 [ms] in duration. Each sub-frame

is further split into two slots, each of 0.5 [ms]. Slots consist of either 6 or 7 OFDM symbols, depending on whether the normal or extended cyclic prefix is employed.

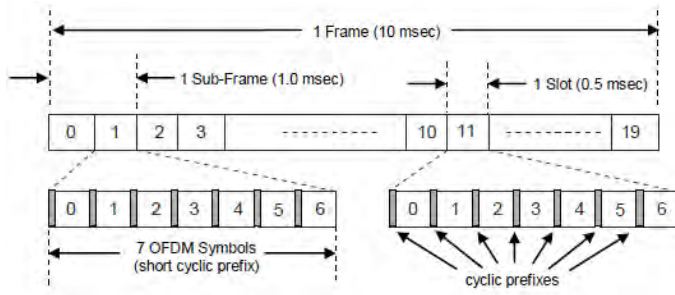


Figure 1 – LTE Generic Frame Structure for FDD Systems.

### B. Random Access Channel and Preamble Sequence Generation

The Random Access Channel (RACH) is an uplink channel primarily used for initial network access and short message transmission, i.e. from UE (User Equipment) to eNodeB (base station). The main purpose of the random access procedure is to obtain uplink time synchronization and to obtain access to the network.

The Physical Random Access Channel (PRACH) preamble, illustrated in Figure 2, consists of a Cyclic Prefix (CP) of length  $T_{CP}$  and a sequence part of length  $T_{PRE}$ .

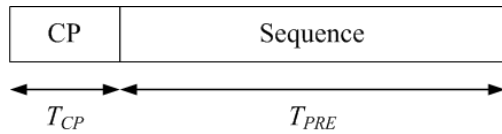


Figure 2 – Random Access Preamble Format.

Prime-length Zadoff-Chu (ZC) sequences are adopted as random access preambles in LTE systems due to its Constant Amplitude Zero Auto Correlation (CAZAC) properties [1, 2], i.e., all points of the sequence lie on the unit circle and its auto-correlation is zero for all time shifts other than zero. These properties make Zadoff-Chu Sequences very useful in channel estimation and time synchronization and also enable improved PRACH preamble detection performance [10].

The 800 [μs] LTE PRACH sequence is built from cyclically-shifting a ZC sequence of prime-length  $N_{ZC}$ , defined as:

$$x_u(n) = \exp \left[ -j \frac{\pi u n (n + 1)}{N_{ZC}} \right], \quad 0 \leq n \leq N_{ZC} - 1 \quad (1)$$

where  $u$  is the ZC sequence index,  $n$  is the time index and the sequence length  $N_{ZC} = 839$  for FDD systems [5]. This sequence length,  $N_{ZC}$ , corresponds to 69.91 Physical Uplink Shared Channel (PUSCH) subcarriers in each SC-FDMA symbol, and offers  $72 - 69.91 = 2.09$  PUSCH subcarriers protection, which corresponds to one PUSCH subcarrier protection on each side of the preamble [5]. Note that the preamble is positioned centrally in the block of 864 available PRACH subcarriers, with 12.5 null subcarriers on each side. Figure 3 depicts the

PRACH preamble mapping according to what was just exposed.

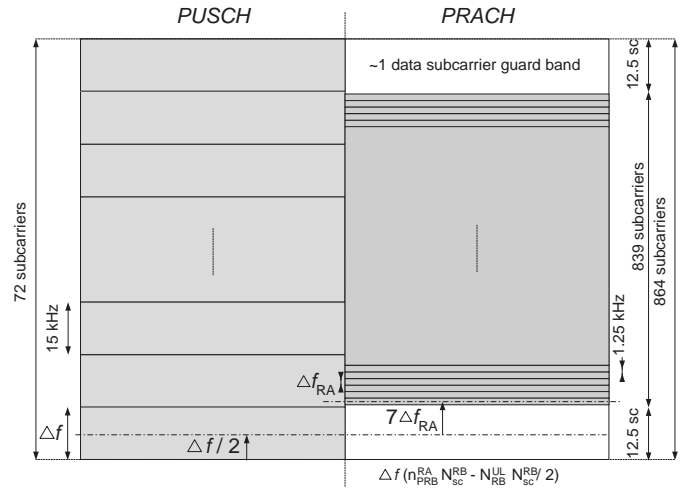


Figure 3 – PRACH preamble mapping onto allocated subcarriers [10].

From the  $u$ th root ZC sequence, random access preambles with zero correlation zones of length  $N_{CS} - 1$  are defined by cyclic shifts according to:

$$x_{u,v}(n) = x_u((n + C_v) \bmod N_{ZC}) \quad (2)$$

where  $N_{CS}$  gives the fixed length of the cyclic shift,  $v$  is the sequence index and  $C_v$  is the cyclic shift applied to the root ZC sequence. These parameters are defined in [5].

### III. PRACH RECEIVER

In order to reduce the complexity, especially for the number of multiplications of the detector at eNodeB, frequency domain processing has been chosen for the preamble detection [10]. The received signal is first pre-processed in time domain, then transformed to the frequency domain by the FFT block and multiplied with the Fourier transformed RACH sequence. The cross correlation is obtained by transforming the multiplication result back to time domain, which is performed by the IFFT and zero-padding blocks. Figure 4 describes the main components of the RACH preamble detector, using a DFT-based (frequency-domain) SC-FDMA receiver [11].

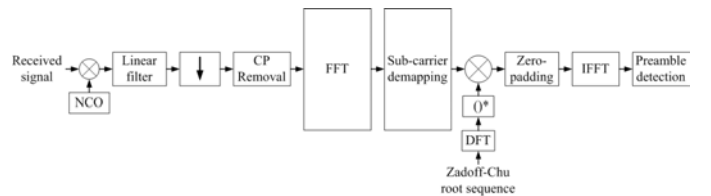


Figure 4 – RACH preamble SC-FDMA receiver structure.

The first block in Figure 4 represents a down-converter, which shifts the PRACH pass-band signal to base-band. After down-converting the signal, the linear filter is applied in order to avoid aliasing after decimation. The result of the decimation block is fed into the CP removal block. After removing the

Cyclic Prefix, the FFT engines transform the SC-FDMA symbols from time domain into frequency domain. The sub-carrier de-mapping block extracts the RACH preamble sequence from the output of the FFT engine. The result of sub-carrier de-mapping is multiplied by the ZC root sequence and then fed into a zero-padding block. Finally, the IFFT engine transforms the cross-correlation result from frequency domain into time domain. The energy detection block estimates noise power, sets the detection threshold and then decides if a preamble is present. For further information on this receiver, refer to [10].

#### A. Power Delay Profile Computation

The LTE PRACH receiver can benefit from the PRACH format and CAZAC properties as described in [11] by computing the PRACH Power Delay Profile (*PDP*) through a frequency-domain periodic correlation. The *PDP* of the received sequence is given by:

$$PDP(l) = |z_u(l)|^2 = \left| \sum_{n=0}^{N_{ZC}-1} y(n)x_u^*[(n+l)_{N_{ZC}}] \right|^2 \quad (3)$$

where  $z_u(l)$  is the discrete periodic correlation function at time lag  $l$  between the received sequence  $y(n)$  and the locally generated root ZC sequence  $x_u(n)$  where  $(\cdot)^*$  denotes the complex conjugate. Both sequences are of length  $N_{ZC}$ . It is worth noticing that by making use of the properties of the DFT,  $z_u(l)$  can efficiently be computed in the frequency domain.

The fact that different PRACH signatures are generated from cyclic shifts of a common root sequence means that the frequency-domain *PDP* computation of a root sequence provides in a one-shot the concatenated *PDP*s of all signatures derived from the same root sequence [10]. Therefore, the signature detection process consists in searching the *PDP* for peaks above a given detection threshold over a search window which corresponds to the cell size.

### IV. PROPOSED PREAMBLE DETECTION METHOD

The energy measurement and the collected data processing are performed in base-band by a device with the architecture depicted in Figure 4. The detection method proposed here is carried out in two stages making use of the *PDP* samples.

The preamble detection procedure consists basically of hypothesis tests following the Neyman&Pearson lemma [17]. This lemma establishes that detectors based on likelihood ratio tests:

$$\frac{PDP_{H_1}}{PDP_{H_0}} > \gamma \quad (4)$$

where the hypothesis  $H_0$  is rejected in favor of  $H_1$  when the desired signal (preamble) is present, is optimum when the cumulative distribution function (CDF) of this ratio given the hypothesis  $H_0$  is known, so that it is possible to calculate the threshold  $\gamma$  that satisfies:

$$P \left\{ \frac{PDP_{H_1}}{PDP_{H_0}} > \gamma \mid H_0 \right\} = P_{FR} \quad (5)$$

for a given false rejection probability  $P_{FR}$ . Typically, the derivation of this function assumes the knowledge of the probability distribution function of both random variables  $PDP_{H_1}$  and  $PDP_{H_0}$ .

The method proposed in this paper is composed of two stages. The first stage is used to identify *PDP* samples that can be considered as containing only the presence of noise, i.e., energy samples, which better represent the hypothesis  $H_0$ . These energy samples must be identified in order to calculate the decision threshold  $\gamma$  of the hypothesis test in the next stage.

The next stage makes use of both the decision threshold  $\gamma$  and the energy of the reference samples to test each one of the *PDP* samples. This procedure makes it possible to reliably decide if there is signal being transmitted on the PRACH channel.

#### A. Censoring Algorithm

The censoring algorithm adopted in this paper is known as Forward Consecutive Mean Excision (FCME) [16]. The basic principle of the algorithm consists in sorting the *PDP* samples in ascending order of energy.

$$\{PDP(i) \mid i = 0, 1, \dots, N_{ZC} - 1\} \quad (6)$$

which results in the ordered set:

$$\{PDP^{(i)} \mid i = 0, 1, \dots, N_{ZC} - 1\} \quad (7)$$

where,

$$PDP^{(0)} < PDP^{(1)} < PDP^{(2)} < \dots < PDP^{(N_{ZC}-1)} \quad (8)$$

Then it discards all samples with energy greater than  $PDP^{(l)}$  such that:

$$PDP^{(l)} > \tau_l \sum_{i=0}^{l-1} PDP^{(i)} \quad (9)$$

where  $\tau_l$  is the censoring scaling factor at the  $l$ th step.

The algorithm used to search for  $PDP^{(l)}$  is performed iteratively, being necessary to calculate the censoring scaling factor  $\tau_l$  for each iteration. The scale factor calculation is done under the initial assumption that  $PDP^{(l)}$  is a *PDP* sample that only contains noise, i.e., free of the presence of signal. Under this assumption, the probability that this test is true corresponds to a probability of false disposal  $P_{FD}$  given by

$$P_{FD} = P \left\{ PDP^{(l)} > \tau_l \sum_{i=0}^{l-1} PDP^{(i)} \mid H_0 \right\} \quad (10)$$

where  $P_{FD}$  is a predefined constant. Each iteration starts with  $I$  equal to the size of the smallest assumed clean set of  $PDP$  samples. The larger the smallest assumed clean set is the better censoring works. However, if the assumed clean set is too large, the probability that corrupted samples will be part of the initial clean set increases. The iteration procedure continues until the test in eq. (9) is true for some value of  $I$  or all the reference samples are decided to be signal-free [15].

As the quadrature components of the correlation signal  $z_u(l)$  present Gaussian distribution with zero mean and variance equal to  $N_{ZC}\sigma^2/2$ , the  $PDP$  samples, consequently, present a non-central Chi-squared distribution with 2 degrees of freedom and mean given by [10]

$$E[PDP^{(i)}] = N_{ZC}\sigma^2 \quad (11)$$

Equivalently, each  $PDP$  sample presents an exponential distribution that is a special case of the Chi-square distribution. Furthermore, since:

$$\sum_{i=0}^{I-1} PDP^{(i)} \approx I E[PDP^{(i)}] \quad (12)$$

Then the equation for the probability of false disposal  $P_{FD}$  can be approximated by:

$$P_{FD} = P\{PDP^{(l)} > \tau_I I N_{ZC}\sigma^2\} \quad (13)$$

This approach becomes better as the set of reference samples  $I$  increases. Therefore, the probability of false disposal  $P_{FD}$  can be approximated by:

$$P_{FD} = e^{-\tau_I I} \quad (14)$$

The probability of false disposal  $P_{FD}$  can be viewed as the desired clean sample rejection rate. Samples that have value above the threshold are discarded and then the new set consists of the remaining samples. The output of the censoring (disposal) stage is then defined by the total energy of the noise reference samples, which is then calculated by:

$$PDP_{ref} = \sum_{i=0}^{I-1} PDP^{(i)} \quad (15)$$

and also by the number of  $PDP$  samples  $I$  employed to calculate  $PDP_{ref}$ .

### B. Detection Procedure

After defining the set of reference samples containing only noise, the next stage consists in testing each  $PDP$  sample against  $PDP_{ref}$ , which is performed through evaluation of the following hypothesis test:

$$PDP(l) \geq \gamma PDP_{ref}, \quad \text{for } l = 0, 1, \dots, N_{ZC} - 1 \quad (16)$$

where  $\gamma$  is the detection threshold which is determined by the decision method employed. Herein the Cell Averaging (CA) method is employed to calculate the detection threshold  $\gamma$  [15].

The detection threshold  $\gamma$  is calculated under the hypothesis of signal absence, i.e., the reference samples contain only noise, for a given probability of false alarm  $P_{FA}$  defined as:

$$P_{FA} = P\left\{\frac{PDP(l)}{PDP_{ref}} > \gamma \mid H_0\right\} \quad (17)$$

Once it is assumed that the quadrature components of the  $PDP$  have Gaussian distribution, therefore in consequence, the energy measures  $PDP(l)$  and  $PDP_{ref}$  present non-central Chi-square distribution with 2 (exponential distribution) and  $2I$  degrees of freedom, respectively. Given that the ratio between two Chi-square distributions results in a Fisher distribution whose cumulative distribution function is given by:

$$FCDF(\gamma) = 1 - P\left\{\frac{PDP(l)/2}{PDP_{ref}/2I} > I\gamma\right\} \quad (18)$$

then the detection threshold  $\gamma$  is calculated by

$$\gamma = FCDF^{-1}(1 - P_{FA}, 2, 2I)/I \quad (19)$$

where  $FCDF$  is the Fisher Cumulative Distribution Function.

After calculating the detection threshold  $\gamma$ , the final decision is made evaluating the test given by eq. (16). If the test is true, signal(s)-plus noise hypothesis  $H_1$  is chosen, i.e., a user is requesting access. Otherwise, the noise-only hypothesis  $H_0$  is decided to be true.

## V. NUMERICAL RESULTS

The threshold given by the method proposed here is found via computer simulations. The number of Monte Carlo runs was greater than  $10^5$  iterations. The ideal AWGN channel is assumed. During the simulations, a user is said present when the energy of a given  $PDP$  sample is greater than the estimated threshold. In this paper, the initial set size for the censoring stage is made equal to 25% of  $N_{ZC}$ , which is the reference set.

For the results presented here, the probability of false alarm  $P_{FA}$  is made equal to  $10^{-4}$  and the probability of false disposal  $P_{FD}$  is made equal to  $10^{-3}$  and therefore, evaluating equation (14) results that the value for  $\tau_I I = T_{CME}$  is 6.9078.

Figure 5 shows the simulated detection probability for one signature generated from one ZC root sequence when the SNR varies from -30 [dB] up to 30 [dB]. It can be noticed that for SNR values greater than -20 [dB], the probability of correct detection is 1, i.e., the presence of a preamble is always detected.

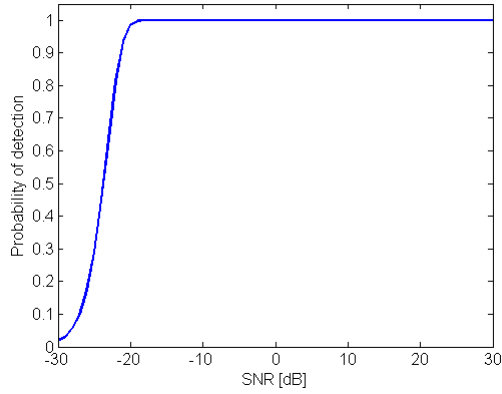


Figure 5 – Simulated detection probability.

Figure 6 depicts the corresponding false alarm probability when the SNR varies from -30 [dB] up to 30 [dB]. It can be noticed that  $P_{FA}$  varies from approximately  $1.03 \times 10^{-4}$  up to  $1.1 \times 10^{-4}$ , showing that the method keeps  $P_{FA}$  close the value set previously for that parameter.

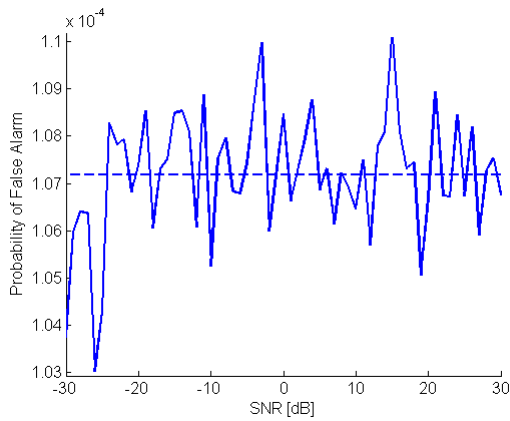


Figure 6 – Simulated false alarm probability.

A comparison between the desired  $P_{FA}$ , which is varied from  $1 \times 10^{-5}$  up to  $1 \times 10^{-4}$ , and the value achieved by the proposed method is presented in Figure 7. As can be noticed, the achieved  $P_{FA}$  value stays rather close to the desired one.

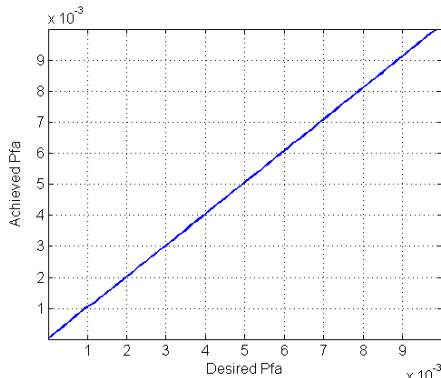


Figure 7 - Comparison between the desired  $P_{FA}$  and the actually achieved value, where SNR = 0 [dB].

Figure 8 shows  $P_D$  versus  $P_{FA}$  (ROC plot). In that figure  $P_{FA}$  is also varied from  $1 \times 10^{-5}$  up to  $1 \times 10^{-4}$  with SNR equal to 0 [dB]. It shows an ideal ROC curve where the presence of a user is always detected independently of the value of  $P_{FA}$ .

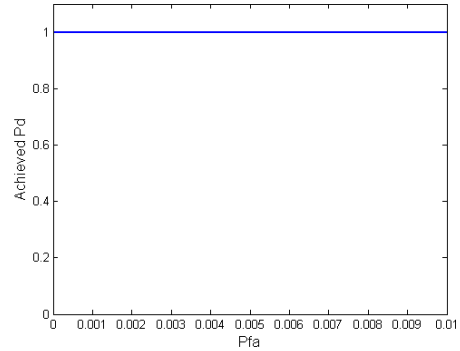


Figure 8 - ROC plot showing  $P_D$  versus  $P_{FA}$  with SNR = 0 [dB].

The proposed method achieves better performance than the methods presented in [18] and [19], where the probabilities of false alarm,  $P_{FA}$ , are  $5 \times 10^{-3}$  and  $10^{-4}$  respectively. The only drawback presented by the method is its moderate to high computational complexity due to the sorting procedure, to the iterative search for a reference set containing only noise and to the test procedure which checks each one of the  $PDP$  samples for the presence of the desired signal. This drawback increases the time the method takes to detect the presence of a user and may impose a constraint to both the number of users it can simultaneously detect and the cell size depending on the architecture the method is implemented.

## VI. CONCLUSION

A modified CA-CFAR method was proposed in this paper. Its main goal is to detect CAZAC sequences that are sent by UEs in order to request the allocation of resources. The numerical results showed that the modified iterative CA-CFAR method proposed here could detect the presence of a user even in the case of SNR as low as -17 [dB]. Also, as the results presented here show that the proposed method does well even in low SNR environments it could be suitable for cognitive radios.

Future work will concentrate on investigations to improve the performance and decrease the computational complexity presented by the proposed method allowing it to be easily implemented in any architecture. Additionally, the influence of the use of antenna diversity over the performance of the method will be assessed as well.

## ACKNOWLEDGMENT

This work was supported by Funttel project "RASFA-4G" at CPQD Telecom and IT Solutions.

## REFERENCES

- [1] R. L. Frank, S. A. Zadoff and R. Heimiller, "Phase shift pulse codes with good periodic correlation properties," IRE Transactions on Information Theory, Vol 7, pp.254-257, October 1961.

- [2] David C. Chu, "Polyphase codes with good periodic correlation properties" *IEEE Transactions on Information Theory*, pp. 531-532, July 1972.
- [3] Mansour, M. M., "Optimized architecture for computing Zadoff-Chu sequences with application to LTE," *GLOBECOM 2009*. IEEE, Nov. 30 2009-Dec. 4, pp. 1-6, 2009.
- [4] 3GPP TS 36.213, "Physical layer procedures (Release 8)", September 2009.
- [5] 3GPP TS 36.211, "Physical Channels and Modulation (Release 8)", September 2009.
- [6] 3GPP TSG RAN WG1 Meeting #44bis, R1-060998, Ericsson, "E-UTRA Random Access Preamble Design", March 2006.
- [7] P. P. Gandhi and S. A. Kassam, "Analysis of CFAR processors in nonhomogeneous background," *IEEE Trans. Aerosp. Electron. Syst.*, vol. 24, no. 4, pp. 427-445, Jul. 1988.
- [8] 3GPP, "LTE Overview", <http://www.3gpp.org/LTE>, accessed on November 1, 2012.
- [9] J. Zyren, "Overview of the 3GPP Long Term Evolution Physical Layer", 2007.
- [10] Stefania Sesia, Issam Toufik and Matthew Baker, "LTE - The UMTS Long Term Evolution: From Theory to Practice", John Wiley & Sons, 2011.
- [11] 3GPP TSG RAN WG1 Meeting #46bis, R1-062630, Texas Instruments, "Non-synchronized Random Access structure for E-UTRA", October 2006.
- [12] T. Yucek, H. Arslan, "A survey of spectrum sensing algorithms for cognitive radio applications", *IEEE Communications Surveys & Tutorials*, v.11 n.1, p.116-130, January 2009.
- [13] M. Barkat, S. D. Himonas, and P. K. Varshney, "CFAR detection probabilities for multiple target situations," in *Proc. Inst. Elect. Eng.*, vol. 136, Oct. 1989, pp. 194-209.
- [14] S. D. Himonas and M. Barkat, "Automatic censored CFAR detection for nonhomogeneous environments," *IEEE Trans. Aerosp. Electron. Syst.*, vol. 28, no. 1, pp. 286-304, Jan. 1992.
- [15] Janne J. Lehtomäki, Markku Juntti and Harri Saarnisaari, "CFAR Strategies for Channelized Radiometer", *IEEE Signal Processing Letters*, Vol. 12, No. 1, January, 2005.
- [16] Janne J. Lehtomäki, Johanna Vartiainen, Markku Juntti and Harri Saarnisaari, "Spectrum sensing with forward methods," in *Proc. IEEE Military Commun. Conf.*, pp. 1-7, Washington, D.C., USA, Oct. 2006.
- [17] J. Neyman and E. S. Pearson, "On the problem of the most efficient tests of statistical hypotheses", *Philosophical Transactions of the Royal Society of London, Series A*. 231: 289-337, 1933.
- [18] Marjan Mazrooei Sebdani and M. Javad Omid, "Detection of an LTE Signal Based on Constant False Alarm Rate Methods and Constant Amplitude Zero Autocorrelation Sequence", *International Conference on Intelligent and Advanced Systems (ICIAS)*, Kuala Lumpur, Malaysia, Jun. 2010.
- [19] Asier Freire-Irigoyen, Rodolfo Torrea-Duran, Sofie Pollin, Min Li, Eduardo Lopez and Liesbet Van der Perre, "Energy Efficient PRACH Detector Algorithm in SDR for LTE Femtocells", *18th IEEE Symposium on Communications and Vehicular Technology (SCVT)*, Nov. 201